

Picosecond Time-Resolved Stokes and Anti-Stokes Raman Studies on the Photochromic Reactions of Diarylethene Derivatives

Chie Okabe,[†] Takakazu Nakabayashi,[‡] Nobuyuki Nishi,[§] Tuyoshi Fukaminato,^{||} Tsuyoshi Kawai,^{||} Masahiro Irie,^{||} and Hiroshi Sekiya^{*,†}

Department of Chemistry, Faculty of Science, Kyushu University, Hakozaki 6-10-1, Higashi-ku, Fukuoka 812-8581, Japan, Research Institute for Electronic Science, Hokkaido University, Sapporo 060-0812, Japan, Institute for Molecular Science, Myodaiji, Okazaki 444-8585, Japan, and Department of Chemistry and Biochemistry, Graduate School of Engineering, Kyushu University, 6-10-1 Hakozaki, Higashiku, Fukuoka 812-8581, Japan

Received: April 19, 2003

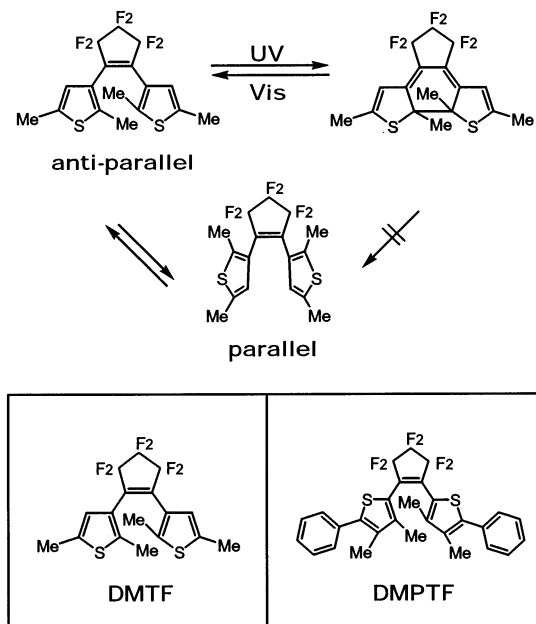
The cyclization and cycloreversion reactions of diarylethene derivatives have been studied with picosecond time-resolved Stokes and anti-Stokes Raman spectroscopies. The cyclization reaction of 1,2-bis(2,5-dimethyl-3-thienyl)perfluorocyclopentene (DMTF) is found to occur within 4 ps to produce the vibrationally excited closed forms in the ground electronic (S_0) state. The time constant of the vibrational relaxation toward a thermal equilibrium with solvent molecules is estimated to be about 10 ps. The cycloreversion reaction of 1,2-bis(3,4-dimethyl-5-phenyl-2-thienyl)perfluorocyclopentene (DMPTF) also generates the vibrationally excited open forms in the S_0 state within 4 ps, which decay on a picosecond time scale. The picosecond time-resolved anti-Stokes Raman spectra of DMPTF show two vibrational bands assignable to the C=C stretching modes of the cyclopentene and thiophene moieties of the generated open forms. The Raman intensity arising from the cyclopentene moiety relative to that from the thiophene moiety becomes smaller with the delay time, indicating that part of the excess energy generated via the cycloreversion reaction is localized on the C=C stretching mode of the cyclopentene moiety. This result suggests that the C=C stretching mode of the cyclopentene moiety is one of the promoting or the accepting modes in the cycloreversion reaction.

1. Introduction

Photochromism is characterized by a light-induced reversible reaction of a chemical species. This reaction gives rise to the formation of photoisomers whose electronic absorption spectra are distinguishably different from that of the reactant molecule, which results in the dramatic color change. Changes in other molecular properties such as reflective and dielectric constants can also occur during the photochromic reaction. The back reaction is induced mostly by a thermal mechanism,^{1,2} whereas some photochromic molecules yield thermally stable photo-products.^{3–9} For such systems, back reactions are photochemical. These phenomena have received much attention in recent years because of their potential applications in optoelectronic devices. Knowledge on the vital factors governing photochromic reactions is essential for designing new photochromic molecules for optical applications.

Diarylethene derivatives are promising photochromic compounds for optical applications because of their thermal irreversibility,^{5–9} fatigue-resistance,^{6,7,9} rapid response,^{9–19} and high sensitivity.²⁰ The photochromic reaction scheme of diarylethene derivatives is shown in Scheme 1. The open forms of diarylethenes are mostly colorless and turn to the closed forms by UV irradiation (cyclization reaction). The generated closed forms are thermally stable and exhibit absorption spectra in the visible region. Upon irradiation of visible light, the closed forms

SCHEME 1



revert back to the original open forms (cycloreversion reaction). From NMR^{6,7,21} and absorption measurements,²¹ it is proved that the open form in solution has at least two rotational conformers: antiparallel and parallel conformers depicted in Scheme 1. The conrotatory cyclization reaction cannot proceed from the parallel conformer. Thus, it can be considered that the

* To whom correspondence should be addressed.

[†] Department of Chemistry, Kyushu University.

[‡] Hokkaido University.

[§] Institute for Molecular Science.

^{||} Department of Chemistry and Biochemistry, Kyushu University.

cyclization yield depends on the ratio of the antiparallel and parallel conformers.

Recently, theoretical calculations have been carried out for a detailed understanding of the reaction dynamics of diarylethene derivatives.^{22,23} Ab initio MCSCF calculations have suggested that the internuclear distance between the reactant carbon atoms in the lowest excited singlet (S_1) state is one of the vital factors governing the cyclization quantum yield. This means that the cyclization yield of diarylethenes depends on the internuclear distance as well as the population of the antiparallel conformer. This result is consistent with the experimental fact that the cyclization yield does not correlate with the population of the antiparallel conformer in some cases.²²

The photoexcitation processes of diarylethene derivatives have been studied with time-resolved techniques.^{10–19} Miyasaka and co-workers have applied picosecond transient absorption and fluorescence techniques to the diarylethene photochromic reactions. The cyclization and cycloreversion reactions of 1,2-bis-(2,4,5-trimethyl-3-thienyl)maleic anhydride (TMTMA) were found to proceed within 10 ps.¹⁰ The cyclization reaction was strongly suppressed in acetonitrile, which was ascribed to the stabilization of nonreactive intermediate states in polar solvents. Recently, the solvent viscosity effect on the photochromism of TMTMA has been investigated.¹³ The yield for the cyclization decreased with increasing solvent viscosity, whereas that for the cycloreversion was almost independent of the solvent viscosity. The rapid (<12 ps) reaction channel of the cyclization of 1,2-bis(2,5-dimethyl-3-thienyl)perfluorocyclopentene (DMTF) has been observed in solution and crystalline phases.¹¹ Tamai et al. have studied the cyclization dynamics of a thiophene oligomer with a diarylethene structure by femtosecond time-resolved absorption spectroscopy.¹⁴ They observed the absorption due to the intermediate state immediately after photoexcitation (<100 fs) and estimated the time constant of the cyclization reaction from this intermediate state to be 1.1 ps. Ern and co-workers have reported that the cyclization reaction of 1,2-bis(2-methyl-3-thienyl)perfluorocyclopentene proceeds within 1.9 ps.¹⁵

Vibrationally resolved spectra have the potential for distinguishing coexisting species from each other in solvents. Recently, we have reported the FT-Raman spectra of 1,2-bis(3-methyl-2-thienyl)perfluorocyclopentene in acetonitrile.²⁴ The Raman bands in the 1400–1600 cm^{-1} region of the open forms are clearly distinguished from those of the closed forms. The vibrational assignments were also performed by density functional theory (DFT) calculations at the B3LYP/6-31G** level. The FT-Raman spectroscopic study suggests that time-resolved vibrational spectroscopy is a promising method for investigating structural changes of the molecule during the photochromic reaction process. To our knowledge, however, no one has reported time-resolved Raman spectra of diarylethenes, primarily because of the difficulty in obtaining two broadly tunable picosecond pulses applicable to time-resolved Raman spectroscopy.

We have recently constructed a two-color independently tunable Raman spectrometer with a time resolution of 4 ps.^{25,26} By using this Raman spectrometer, we have studied the cyclization and cycloreversion reactions of diarylethene derivatives in solutions. The resonance Stokes and anti-Stokes Raman spectra of the open and closed forms generated during the photochromism has been observed. These vibrational spectra reflect configurational changes and vibrational relaxation of the generated photoisomers. We have used DMTF and 1,2-bis(3,4-

dimethyl-5-phenyl-2-thienyl)perfluorocyclopentene (DMPTF) in this study. These chemical structures are depicted in Scheme 1.

2. Experimental Section

The spectrometer for time-resolved Raman measurements was already described elsewhere.^{25,26} A beam from a regenerative amplifier (Quantronix, Taitan, wavelength 790 nm, repetition rate 1 kHz, pulse energy 2.8 mJ, pulse duration 4 ps) was used to excite two optical parametric amplifier systems (Light Conversion, TOPAS). By using sum- and difference frequency mixings, we obtained the continuous tuning of light between 189 and 11 200 nm with keeping microjoule pulse energy. The outputs from the two OPA systems were used as the pump beam for exciting photochromic molecules and the probe beams for resonance Raman observation. After passing through fixed (for the pump beam) and variable (for the probe beam) optical delay lines, the pump and probe beams were focused noncollinearly onto the sample with an $f = 100$ mm lens. The sample solution was flowed through a squeezed stainless steel nozzle to form a thin (~ 0.3 mm) liquid jet. The polarization of the pump beam was rotated by 54.7° relative to that of the probe beam to ensure the observed kinetics free from the effects of molecular rotations. The instrumental function was determined by a sum-frequency mixing between the outputs from the two OPA systems. It was estimated to be a Gaussian function with a full width at half-maximum of 4 ps.

The 90° -scattered Raman signal was collected and dispersed by a single spectrograph (JOBIN YVON-SPEX, 500MS) and detected by a liquid-nitrogen-cooled CCD camera (Princeton Instruments, LN/CCD-1340PB, 1340×400 pixels). The unshifted scattered light was rejected with a holographic notch filter (Kaiser Optical Systems) and/or a color glass filter (SIGMA KOKI) placed in front of the entrance slit of the spectrograph. The spectral slit width was ~ 10 cm^{-1} . In a series of measurements, the order of the delay time was set to be random to minimize effects of long-term drifts of the laser system on the observed data. The typical exposure time was 200 s. The spectra reported here were taken by the average of the data for 10–30 cycles. The pump-only and probe-only spectra were subtracted from the pump–probe spectra, providing the spectra due to transients. Emission lines from a neon lamp and solvent Raman bands were used to calibrate the transient Raman spectra.

DMTF was synthesized and purified as reported previously.⁸ Synthesis method of DMPTF is described in the Appendix. Solvents (Wako Pure Chemical Industries, special reagent grade) were used as received. The concentration of the sample solution was $1 \times 10^{-3} \sim 5 \times 10^{-4}$ mol dm^{-3} . All experiments were carried out at room temperature (295 K).

3. Results

3.1. Time-Resolved Stokes Raman Spectra of DMTF.

Figure 1 shows the electronic absorption spectra of the open and closed forms of DMTF in 1-butanol. The open forms are almost colorless, and their electronic absorption intensities start from the UV region (<360 nm), whereas the closed forms generated by UV irradiation show the absorption in the visible region. Figure 2A shows the picosecond time-resolved Stokes Raman spectra on excitation of the open forms of DMTF in 1-butanol. Raman bands of the solvent and fluorescence from the open forms are subtracted in these spectra. The pump and probe wavelengths are 310 and 568 nm, respectively. The probe wavelength of 568 nm is in resonance with the absorption of

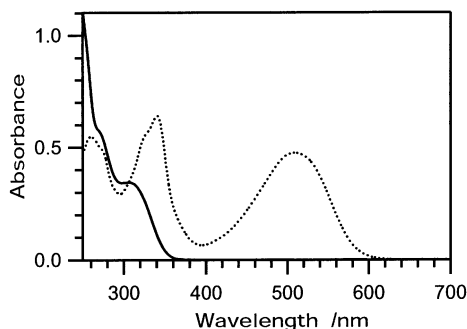


Figure 1. Electronic absorption spectra of open and closed forms of DMTF in 1-butanol solution. Solid line, open form; dotted line, closed form.

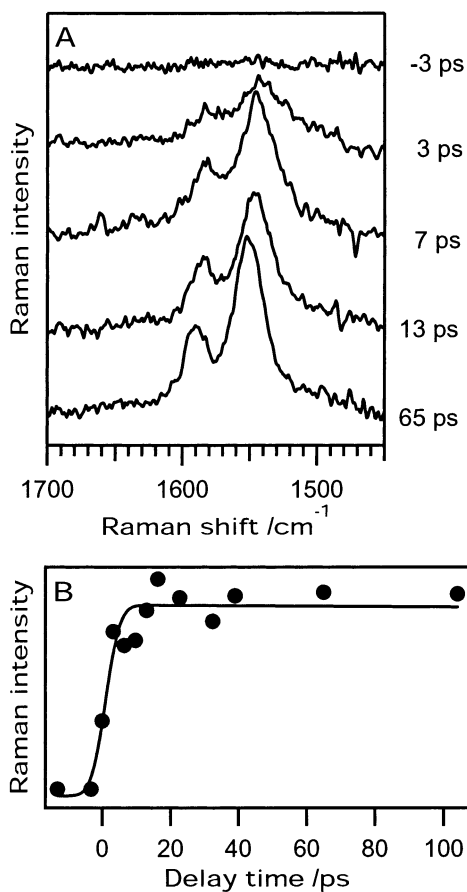


Figure 2. (A) Picosecond time-resolved Stokes Raman spectra of DMTF in 1-butanol. Pump, 310 nm; probe, 568 nm. The delay time is given on the right-hand side of each spectrum. (B) Temporal intensity change of the transient Raman band at 1551 cm^{-1} . The solid curve is the fit to the data by the convolution of the instrumental function with a nanosecond decay function.

the closed forms in Figure 1. The peak positions and the intensity ratios of the two bands at 1551 and 1592 cm^{-1} in Figure 2A are almost the same as those of the bands observed in cw resonance Raman spectra of the closed forms. These two bands disappear with the probe wavelengths off resonance with the visible absorption of the closed forms. Thus, the observed two Raman bands in Figure 2A can be ascribed to the closed forms in the S_0 state generated via the cyclization.

Figure 2B shows the time-development of the integrated intensity of the Raman band at 1551 cm^{-1} . The time-resolved curve rises within the experimental temporal resolution (<4 ps) and then remains almost unchanged for delay times >10 ps. The intensity of the 1592 cm^{-1} band also shows a very similar

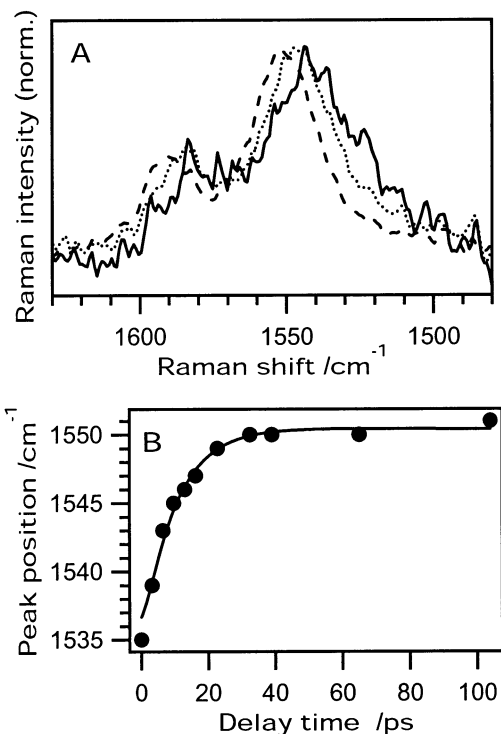


Figure 3. (A) Time dependence of the Stokes Raman bands of the generated closed forms of DMTF in 1-butanol. The intensity scale is normalized for the peak intensities of the respective spectra. Solid trace, 3 ps; dotted trace, 13 ps; dashed trace, 65 ps. Pump, 310 nm; probe, 568 nm. (B) Temporal change in the center wavenumber of the Raman band of the closed forms of DMTF at 1551 cm^{-1} . The solid curve represents the best fit to the data by the convolution of the instrumental function with a single-exponential function. The obtained time constant is 10 ps.

behavior. These Raman results lead us to a conclusion that the cyclization reaction of DMTF occurs within 4 ps. The instrumental-limited rise is also observed in ethylene glycol with a high viscosity coefficient. Fluorescence arising from the excited open forms seriously interferes with the observation in the anti-Stokes Raman region. With the probe wavelengths of 568, 632, 670, and 790 nm, we have detected no Raman bands assignable to the transient species in electronically excited states. It has been known that the transient species of DMTF show only weak absorption intensities in the visible and NIR region.¹¹ Because the resonance Raman intensity is proportional to the electronic transition moment to the fourth power, the resonance Raman intensities due to the transient species are not so emphasized as to be detected within our experimental uncertainty.

In Figure 2A, the peak positions and bandwidths of the Raman bands also change with the delay time. Figure 3A shows the time-resolved Raman spectra at delay times 3, 13, and 65 ps. The intensity of each spectrum is roughly normalized by reference to the intensity of the band at 1551 cm^{-1} . The peak positions of the transient Raman bands shift to higher-wavenumbers, and their bandwidths become narrower as the delay time is increased. The center wavenumber of the 1551 cm^{-1} band is plotted against the delay time in Figure 3B. We adopt the first moment analysis to estimate the center wavenumber.²⁵ The peak position at 0 ps delay time is found to be about 16 cm^{-1} lower than that at 65 ps. The observed time profile is satisfactorily reproduced by the convolution of the instrument function with a single-exponential function. The obtained time constant is 10 ps.

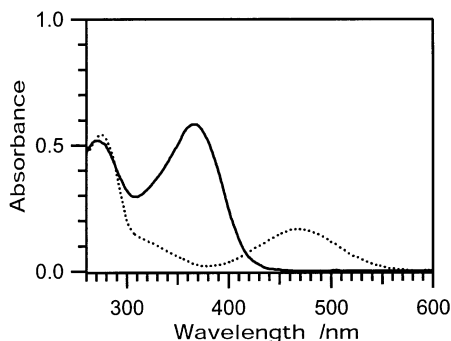


Figure 4. Electronic absorption spectra of open and closed forms of DMPTF in acetonitrile solution. Solid line, open form; dotted line, closed form.

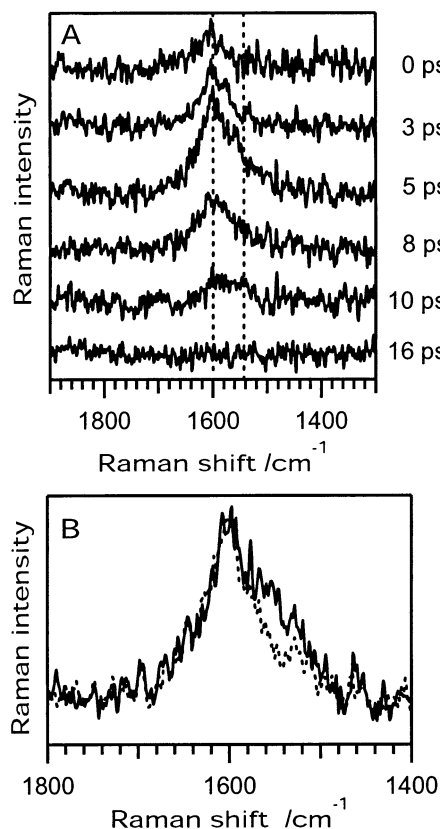


Figure 5. (A) Picosecond time-resolved anti-Stokes Raman spectra of DMPTF in acetonitrile. Pump, 480 nm; probe, 395 nm. Dotted lines indicate the peak positions of the anti-Stokes Raman bands of the open forms of DMPTF in the S_0 state. The delay time is given on the right-hand side of each spectrum. (B) Time dependence of the anti-Stokes Raman bands of the generated open forms of DMPTF in acetonitrile. The intensity scale is normalized for the peak intensities of the respective spectra. Solid trace, 2 ps; dotted trace, 8.5 ps.

3.2. Time-Resolved Anti-Stokes Raman Spectra of DMPTF.

The electronic absorption spectra of the open and closed forms of DMPTF in acetonitrile are shown in Figure 4. The open forms of DMPTF are pale yellow and have the absorption maximum at ≈ 370 nm. The closed forms photogenerated from the open forms are orange and show the visible absorption around 470 nm. Figure 5A shows the picosecond time-resolved anti-Stokes Raman spectra on excitation of the closed forms of DMPTF in acetonitrile. These anti-Stokes Raman spectra arise from only the vibrationally excited transients. Fluorescence from the sample and solvent Raman bands are subtracted. The pump wavelength of 480 nm is near the absorption maximum of the closed forms. The probe wavelength of 395 nm is in resonance

with the absorption due to the open forms. The peak positions of the two bands at 1545 and 1599 cm^{-1} in Figure 5A are almost the same as those of the vibrational bands of the open forms observed by FT-Raman spectroscopy. Thus, the observed two anti-Stokes Raman bands in Figure 5A can be assigned to the vibrationally excited open forms in the S_0 state generated by the photoexcitation of the closed forms. In Figure 5A, the intensities of the anti-Stokes Raman bands rise within the experimental temporal resolution (<4 ps), and then these bands completely disappear at 16 ps delay time. This result indicates that the cycloreversion of DMPTF proceeds within 4 ps and the vibrationally excited open forms are generated as the intermediate state. It is difficult to obtain the reliable Stokes Raman data because of interference by fluorescence from the excited open forms.

As shown in Figure 5A, the relative intensity of the two anti-Stokes Raman bands also changes with the delay time. Figure 5B shows the anti-Stokes Raman spectra at delay times 2 and 8.5 ps. Each spectrum is roughly normalized to the intensity of the 1599 cm^{-1} band. The intensity of the 1545 cm^{-1} band relative to that of the 1599 cm^{-1} band becomes larger as the delay time increases.

4. Discussion

4.1. Cyclization Reaction of DMTF. We first discuss the dynamics of the cyclization reaction of DMTF. As mentioned before, the Stokes Raman intensities due to the photogenerated closed forms show the instrumental-limited rise (<4 ps), indicating the cyclization of DMTF occurs within 4 ps. The changes in the band shape as well as in the band intensity are also important to understand the cyclization process. As shown in Figure 3, the center wavenumbers of the Stokes bands shift upward with a time constant of 10 ps, being accompanied by band narrowing. The high-wavenumber shift and the band narrowing of vibrational bands, which occur on a picosecond time scale, have been observed in other polyatomic molecules in solution. All of the dynamics have been considered to be associated with intermolecular vibrational relaxation of hot solutes toward thermal equilibria with surrounding solvent molecules.^{25–31} Iwata and Hamaguchi have observed the picosecond high-wavenumber shift and the band narrowing of the Raman bands of *trans*-stilbene in the S_1 state.³⁰ The temporal shift of the olefinic C=C stretching band was found to be a good indicator of the temperature change in the solute. For picosecond Raman spectra of nickel octaethylporphyrin, Mizutani et al. have shown that the time constant of the high-wavenumber shift is close to that of vibrational relaxation of the solute toward a thermal equilibrium with solvent molecules.³¹ The peak positions and bandwidths of vibrational bands depend on the temperature of solute molecules; in general, the vibrational bands due to skeletal modes broaden and shift to lower-wavenumbers with increasing temperature. This behavior has been considered to be mainly caused by anharmonic couplings with the bath of low-wavenumber modes.³²

Immediately after the cyclization reaction, the vibrationally excited closed forms in the S_0 state should be generated as an intermediate state. This is because the ultrafast cyclization deposits a large amount of excess energy [in this case, the difference between electronic energies of the photoexcited open forms and the closed forms in the S_0 state] into the vibrational manifold of the photoproducts. The relaxation process from the vibrationally excited states to a thermodynamically favorable state may be hence observed spectroscopically. Generally speaking, it takes several to tens of picoseconds for the

vibrationally excited large molecules to dissipate excess energy into surrounding solvent molecules through intermolecular interactions.^{25–31,33} Thus, the high-wavenumber shift and the band narrowing observed in the present study can be ascribed to the intermolecular vibrational relaxation of the photogenerated closed forms in the S_0 state toward the thermal equilibrium with solvent molecules. The anti-Stokes/Stokes intensity ratios will provide information on vibrational relaxation, however, the difference between the resonance effects of the Stokes and anti-Stokes Raman spectra must be considered in their analysis.

The above result indicates that the cyclization of DMTF occurs within 4 ps and the vibrationally excited closed forms in the S_0 state are generated as the intermediate. The energy dissipation into surrounding solvent molecules occurs with a time constant of 10 ps, generating the thermally equilibrated S_0 closed forms at room temperature.

The activation energy of the cyclization reaction of DMTF should be very small because the cyclization occurs within 4 ps. This result is consistent with the fact that the ultrafast cyclization (<4 ps) is also observed in ethylene glycol with a high viscosity coefficient. However, two fluorescence components with lifetimes of subnanoseconds and a few nanoseconds were observed on the photoexcitation of the open forms of DMTF.¹¹ These components do not arise from the generated closed forms, which are known to show no fluorescence in the nanosecond time range.⁹ Thus, it is considered that the nanosecond fluorescence signals are due to the open forms, although the very rapid cyclization channel (<4 ps) exists in their photoexcited states. Two possible mechanisms can be considered to explain the existence of both the ultrafast and the nanosecond components in the photoexcited open forms as follows.

The optical transition between the S_0 and S_1 states is forbidden by symmetry.^{21–23} Under irradiation of UV light, the open forms are excited to optically allowed, excited singlet state (S_2). Ab initio molecular orbital calculations have suggested that the S_1 molecules formed via the S_2 state have two potential minima: one is a reactive site from which the very rapid cyclization occurs and the other is a nonreactive site. We have observed the fluorescence excitation and dispersed fluorescence spectra of the open forms of 1,2-bis(3-methyl-2-thienyl)perfluorocyclopentene in a supersonic free jet.³⁴ The dispersed fluorescence spectrum was strongly Stokes-shifted with respect to the excitation wavelength, indicating that the optically allowed state is not the S_1 state. The S_1 state may be generated via very fast internal conversion from the S_2 state, providing fluorescence. Thus, the experimental results are consistent with the theoretical ones. Hence, it is considered that the observed subnanosecond and nanosecond fluorescence signals arise from the open forms in the nonreactive site with subnanosecond and nanosecond lifetimes. This means that the cyclization takes place mainly from the reactive site in the S_1 state, whereas the reaction from the nonreactive site may also occur with a low quantum yield. This model is consistent with the work of Miyasaka et al., who have suggested that both the very rapid and slow reaction pathways exist in the cyclization of TMTMA.¹³ They observed the subnanosecond and nanosecond fluorescence signals following the excitation of the open forms of TMTMA and ascribed the subnanosecond component to the intermediate for the slow cyclization and the nanosecond component to the photoexcited parallel conformers which cannot convert to the closed forms. The fluorescence intensity of the nanosecond component was observed to be rather smaller than that of the subnanosecond component, although NMR spectroscopy has suggested that the

parallel and antiparallel conformers exist in almost equal amounts in solution.^{6,7,9} It may be necessary to clarify the large intensity difference between the subnanosecond and nanosecond components, if we assign the subnanosecond fluorescence to the antiparallel conformers and the nanosecond fluorescence to the parallel conformers.

Both the parallel and antiparallel conformers existing in solution are photoexcited on the UV irradiation. Because there is no chance for the parallel conformers to be converted to the closed forms, it is conceivable that the photoexcited parallel conformers have subnanosecond and nanosecond lifetimes and show the observed fluorescence. This means that both the subnanosecond and nanosecond fluorescence signals are due to the photoexcited parallel conformers.

In the present study, we cannot determine which of the two mechanisms proceeds after the photoexcitation of the open forms of DMTF. Measurements with higher temporal resolution are needed to reach a more definitive conclusion on this point.

4.2. Cycloreversion Reaction of DMPTF. In Figure 5A, the anti-Stokes Raman intensities of the photogenerated open forms show the instrumental-limited rise, indicating that the cycloreversion of DMPTF occurs within 4 ps. The excess energy generated via the ultrafast cycloreversion must be initially localized on Franck–Condon active vibrations of the S_0 open forms; the vibrationally excited populations must be greatly different from those under the thermal equilibrium at room temperature. The localized excess energy is then distributed among all intramolecular vibrational modes according to the Boltzmann distribution (intramolecular vibrational relaxation). This intramolecular relaxation creates a quasi-equilibrium among all intramolecular modes, resulting in a single, mode-independent vibrational temperature. As discussed in subsection 4.1, this randomized vibrational energy dissipates to solvent molecules in tens of picoseconds (intermolecular vibrational relaxation).

Time-resolved anti-Stokes Raman spectroscopy is one of the powerful methods for studying vibrational relaxation in solution.^{29,31,34,35} It probes only those molecules that are populated in excited vibrational states, and hence provides state-specific dynamical information that is essential for a detailed understanding of vibrational relaxation. In general, anti-Stokes Raman intensities for high-wavenumber modes are very weak, because of small populations on their vibrationally excited levels at room temperature. In Figure 5A, on the contrary, the anti-Stokes Raman bands for the high-wavenumber modes of the open forms are clearly observed at short delay times. These anti-Stokes Raman intensities decrease with increasing delay time and disappear at 16 ps delay time within the experimental accuracy. The large intensity decrease with the delay time in Figure 5A clearly indicates that the anti-Stokes Raman spectra at short delay times are attributed to the vibrationally excited open forms generated via the cycloreversion. At 16 ps delay time, the photogenerated open forms have almost reached the thermal equilibrium at room temperature. Thus, no transient anti-Stokes Raman signal is observed at 16 ps within our experimental uncertainty.

The relative intensity between the two anti-Stokes bands also changes with the delay time (Figure 5B). It is hard to explain the observed relative intensity change on the basis of the Boltzmann distribution because the energy difference between these bands is only $\approx 54 \text{ cm}^{-1}$. If the Boltzmann distribution of the excess energy is assumed, the single intramolecular vibrational temperature must be higher than 1500 K, which is apparently an unrealistic value. Thus, the observed relative

intensity change reflects the nonstatistical distribution of the excess energy in the generated open forms at short delay times. In view of the temporal resolution of the present experiment, it is concluded that it takes at least several picoseconds for the open forms of DMPTF in the S_0 state to reach the intramolecular thermal equilibrium. In other words, the intramolecular vibrational relaxation does not complete within a few picoseconds. For medium-size to large molecules in solution, an empirical rule that the time scale of intramolecular vibrational relaxation is in the subpicosecond range and that of intramolecular relaxation in tens of picoseconds has been proposed from a number of data on vibrational relaxation.³³ However, recent experiments have suggested that intramolecular relaxation occurs in the time range of several picoseconds in some cases.^{29,31,35–37}

At short delay times, the intensity of the 1599 cm^{-1} band is stronger than that of the 1545 cm^{-1} band. With increasing delay time, the intensity difference between these two bands becomes smaller. This indicates that the excess energy is localized on the 1599 cm^{-1} mode rather than on the 1545 cm^{-1} mode at short delay times. Ab initio DFT calculations have assigned the observed 1545 and 1599 cm^{-1} bands to the C=C stretching modes of the thiophene and the cyclopentene moiety, respectively.²⁴ Thus, it is concluded that the excess energy generated via the cycloreversion is localized on the C=C stretching mode of the cyclopentene moiety of the S_0 open forms of DMPTF. This result indicates that the C=C stretching mode of the cyclopentene moiety is a promoting or an accepting mode in the cycloreversion reaction. This mode can be regarded as one of the vital factors governing the cycloreversion rate.

5. Conclusion

Photochromic reactions of diarylethene derivatives have been studied by picosecond time-resolved Stokes and anti-Stokes Raman spectroscopies. Two common features of the cyclization and cycloreversion reactions are found: the photochromic reactions proceed within 4 ps and the vibrationally excited photoisomers in the S_0 state are generated as the intermediate state. Two anti-Stokes Raman bands at 1545 and 1599 cm^{-1} are observed on photoexcitation of the closed forms of DMPTF. They are assignable to the C=C stretching modes of the thiophene and the cyclopentene moiety of the generated S_0 open forms, respectively. The intensity of the cyclopentene moiety relative to that of the thiophene moiety becomes smaller with the delay time, indicating that part of the excess energy generated via the cycloreversion is localized on the C=C stretching mode of the cyclopentene moiety. This means that the C=C stretching mode of the cyclopentene moiety is one of the promoting or the accepting modes in the cycloreversion reaction. The C=C stretching mode of the cyclopentene moiety is found to be one of the vital factors governing the cycloreversion yield. Finally, we note that time-resolved vibrational spectroscopy provides important information on vibrational relaxation and reaction coordinates, which is difficult to obtain from electronic spectroscopic techniques in condensed phases. This method will give new scope for elucidating the dynamical features of diarylethene photochromism.

Acknowledgment. This work was supported by the Joint Studies Program (2002–2003) of the Institute for Molecular Science.

Appendix

3,4-Dimethyl-2-phenylthiophene. To a solution of 3,4-dimethylthiophene (4.1 g, 36.3 mmol) and N,N,N',N' -tetra-

methylethylenediamine (TMEDA; 6.0 mL, 40 mmol) in anhydrous ether (40 mL) was added dropwise $n\text{-BuLi}$ (1.6 M in hexane, 25 mL, 41 mmol) and stirred for 1 h at $0\text{ }^\circ\text{C}$ under argon atmosphere. After cooling the solution to $-78\text{ }^\circ\text{C}$, tri- n -butyl borate (11.5 mL, 43 mmol) was gradually added and stirred for 2 h. After warming to room temperature, the reaction mixture diluted with anhydrous THF (120 mL). To the solution was added 20 wt % Na_2CO_3 aqueous solution (48 mL), iodobenzene (7.2 g, 35 mmol), $\text{Pd}(\text{PPh}_3)_4$ (2.15 g). The solution was refluxed for 5 h at $70\text{ }^\circ\text{C}$. After the heating was over, the reaction mixture was poured into the water, and the reaction was extracted with ether. The combined organic layer was dried with MgSO_4 , filtered, and evaporated in vacuo. The residue was purified by silica gel column chromatograph (hexane) to give 4.63 g of 3,4-dimethyl-2-phenylthiophene in 68% yield as a colorless liquid: $^1\text{H NMR}$ (200 MHz, CDCl_3) $\delta = 2.19$ (s, 3H), 2.21 (s, 3H), 6.90 (s, 1H), 7.2–7.5 (m, 5H); MS m/z 188 (M^+). Anal. Calcd for $\text{C}_{12}\text{H}_{12}\text{S}$: C, 76.55; H, 6.42. Found: C, 76.38; H, 6.51.

1,2-Bis(3,4-dimethyl-5-phenyl-2-thienyl)perfluorocyclopentene. To a solution containing 4.63 g (24.6 mmol) of 3,4-dimethyl-2-phenylthiophene in 30 mL anhydrous ether (150 mL) was added 16.2 mL (26.6 mmol) of $n\text{-BuLi}$ (1.6 N in hexane solution) at $-5\text{ }^\circ\text{C}$ under an argon atmosphere. After the mixture was heated under reflux for 45 min, the reaction mixture was cooled to $-78\text{ }^\circ\text{C}$. Perfluorocyclopentene (1.62 mL, 12.1 mmol) was added gradually and stirred for 1 h at this temperature. Methanol was added to the reaction mixture and extracted with ether, dried with MgSO_4 , filtered, and evaporated in vacuo. The residue was purified by silica gel column chromatography (hexane) followed by recrystallization from hexane afforded yellow crystals of 1,2-bis(3,4-dimethyl-5-phenyl-2-thienyl)perfluorocyclopentene (2.0 g, 30%): mp $150.1\text{--}150.8\text{ }^\circ\text{C}$; $^1\text{H NMR}$ (200 MHz, CDCl_3) $\delta = 1.75$ (s, 3H), 2.14 (s, 3H), 7.3–7.5 (m, 5H); MS m/z 548 (M^+). Anal. Calcd for $\text{C}_{29}\text{H}_{22}\text{F}_6\text{S}_2$: C, 63.49; H, 4.04. Found: C, 63.27; H, 4.14.

References and Notes

- (1) Hirano, M.; Miyashita, A.; Nohira, H. *Chem. Lett.* **1991**, 209.
- (2) Sachman, E. *J. Am. Chem. Soc.* **1971**, 93, 7088.
- (3) Heller, H. G.; Oliver, S. *J. Chem. Soc., Perkin Trans. 1* **1981**, 197.
- (4) Darcy, P. J.; Heller, H. G.; Strydom, P. J.; Whittall, J. *J. Chem. Soc., Perkin Trans. 1* **1981**, 202.
- (5) Irie, M.; Mohri, M. *J. Org. Chem.* **1988**, 53, 803.
- (6) Uchida, K.; Nakayama, Y.; Irie, M. *Bull. Chem. Soc. Jpn.* **1990**, 63, 1311.
- (7) Hanazawa, M.; Sumiya, R.; Horikawa, Y.; Irie, M. *J. Chem. Soc., Chem. Commun.* **1992**, 206.
- (8) Kobatake, S.; Yamada, T.; Uchida, K.; Kato, N.; Irie, M. *J. Am. Chem. Soc.* **1999**, 121, 2380.
- (9) Irie, M. *Chem. Rev.* **2000**, 100, 1685.
- (10) Miyasaka, H.; Araki, S.; Tabata, A.; Nobuto, T.; Mataga, N.; Irie, M. *Chem. Phys. Lett.* **1994**, 230, 249.
- (11) Miyasaka, H.; Nobuto, T.; Itaya, A.; Tamai, N.; Irie, M. *Chem. Phys. Lett.* **1997**, 269, 281.
- (12) Miyasaka, H.; Murakami, M.; Itaya, A.; Guillaumont, D.; Nakamura, S.; Irie, M. *J. Am. Chem. Soc.* **2001**, 123, 753.
- (13) Miyasaka, H.; Nobuto, T.; Murakami, M.; Itaya, A.; Tamai, N.; Irie, M. *J. Phys. Chem. A* **2002**, 106, 8096.
- (14) Tamai, N.; Saika, T.; Shimidzu, T.; Irie, M. *J. Phys. Chem.* **1996**, 100, 4689.
- (15) Ern, J.; Bens, A. T.; Bock, A.; Martin, H.-D.; Kryschi, C. *J. Lumin.* **1998**, 76/77, 90.
- (16) Ern, J.; Bens, A. T.; Martin, H.-D.; Mukamel, S.; Schmid, D.; Tretiak, S.; Tsiper, E.; Kryschi, C. *Chem. Phys.* **1999**, 246, 115.
- (17) Ern, J.; Bens, A. T.; Martin, H.-D.; Mukamel, S.; Schmid, D.; Tretiak, S.; Tsiper, E.; Kryschi, C. *J. Lumin.* **2000**, 87/79, 742.
- (18) Ern, J.; Bens, A. T.; Martin, H.-D.; Kuldova, K.; Trommsdorff, H. P.; Kryschi, C. *J. Phys. Chem. A* **2002**, 106, 1654.
- (19) Owirutsky, J. C.; Nelson, H. H.; Baronavski, A. P.; Kim, O.-K.; Tsvigouli, G. M.; Gilat, S. L.; Lehn, J.-M. *Chem. Phys. Lett.* **1998**, 293, 555.

- (20) Kawai, T.; Fukuda, N.; Gröschl, D.; Kobatake, S.; Irie, M. *Jpn. J. Appl. Phys.* **1999**, *38*, L1194.
- (21) Goldberg, A.; Murakami, A.; Kanda, K.; Kobayashi, T.; Nakamura, S.; Uchida, K.; Sekiya, H.; Fukaminato, T.; Kawai, T.; Kobatake, S.; Irie, M. to be published.
- (22) Uchida, K.; Guillaumont, D.; Tsuchida, E.; Mochizuki, G.; Irie, M.; Murakami, A.; Nakamura, S. *J. Mol. Struct. (THEOCHEM)* **2002**, *579*, 115.
- (23) Guillaumont, D.; Kobayashi, T.; Kanda, K.; Miyasaka, H.; Uchida, K.; Kobatake, S.; Shibata, K.; Nakamura, S.; Irie, M. *J. Phys. Chem. A* **2002**, *106*, 7222.
- (24) Okabe, C.; Tanaka, N.; Fukaminato, T.; Kawai, T.; Irie, M.; Nibu, Y.; Shimada, H.; Goldberg, A.; Nakamura, S.; Sekiya, H. *Chem. Phys. Lett.* **2002**, *357*, 113.
- (25) Nakabayashi, T.; Kamo, S.; Sakuragi, H.; Nishi, N. *J. Phys. Chem. A* **2001**, *105*, 8605.
- (26) Nakabayashi, T.; Kamo, S.; Watanabe, K.; Sakuragi, H.; Nishi, N. *Chem. Phys. Lett.* **2002**, *355*, 241.
- (27) Butler, R. M.; Lynn, M. A.; Gustafson, T. L. *J. Phys. Chem.* **1993**, *97*, 2609.
- (28) Hester, R. E.; Matousek, P.; Moore, J. N.; Parker, A. W.; Toner, W. T.; Towrie, M. *Chem. Phys. Lett.* **1993**, *208*, 471.
- (29) Qian, J.; Schultz, S. L.; Jean, J. M. *Chem. Phys. Lett.* **1995**, *233*, 9.
- (30) Iwata, K.; Hamaguchi, H. *J. Phys. Chem. A* **1997**, *101*, 632.
- (31) Mizutani, Y.; Uesugi, Y.; Kitagawa, T. *J. Chem. Phys.* **1999**, *111*, 8950.
- (32) Asher, S. A.; Murtaugh, J. *J. Am. Chem. Soc.* **1983**, *105*, 7244.
- (33) Elsaesser, T.; Kaiser, W. *Annu. Rev. Phys. Chem.* **1989**, *40*, 143.
- (34) Tanaka, N.; Okabe, C.; Sakota, K.; Fukaminato, T.; Kawai, T.; Irie, M.; Goldberg, A.; Nakamura, S.; Sekiya, H. *J. Mol. Struct.* **2002**, *616*, 113.
- (35) Nakabayashi, T.; Okamoto, H.; Tasumi, M. *J. Phys. Chem. A* **1998**, *102*, 9686.
- (36) Shreve, A. P.; Mathies, R. A. *J. Phys. Chem.* **1995**, *99*, 7285.
- (37) Lenz, K.; Pfeiffer, A.; Lau, A.; Elsaesser, T. *Chem. Phys. Lett.* **1994**, *229*, 340.